CJC Chinese Journal of Chemistry
中国化学 - An International Journal

Check for updates

Accepted Article

Title: Synthesis, Bioactivity Evaluation, 3D-QSAR, and Molecular Docking of Novel Pyrazole-4-carbohydrazides as Potential Fungicides Targeting Succinate Dehydrogenase

Authors: Jian Jiao, Min Chen, Shengxin Sun, Weijie Si, Xiaobin Wang, Weijie Ding, Xincan Fu, An Wang, Chunlong Yang*

This work may now be cited as: *Chin. J. Chem.* **2020**, *38,* 10.1002/cjoc.202000438.

The final Version of Record (VoR) of it with formal page numbers will soon be published online in Early View: http://dx.doi.org/10.1002/cjoc.202000438.

WILEY-VCH SIOC CCS

ISSN 1001-604X • CN 31-1547/O6
mc.manuscriptcentral.com/cjoc
www.cjc.wiley-vch.de

Report | Pyrazole, Carbohydrazides, Antifungal evaluation, 3D-QSAR, Molecular docking | CJC Chinese Journal of Chemistry 中国化学 - An International Journal

Synthesis, Bioactivity Evaluation, 3D-QSAR, and Molecular Docking of Novel Pyrazole-4-carbohydrazides as Potential Fungicides Targeting Succinate Dehydrogenase

Jian Jiao, Min Chen, Shengxin Sun, Weijie Si, Xiaobin Wang, Weijie Ding, Xincan Fu, An Wang, Chunlong Yang*

Jiangsu Key Laboratory of Pesticide Science, College of Sciences , Nanjing Agricultural University, Nanjing, 210095, China.

Cite this paper: *Chin. J. Chem.* **2019**, *37*, XXX—XXX. **DOI: 10.1002/cjoc.201900XXX**

Summary of main observation and conclusion To screen novel antifungal agents targeting the succinate dehydrogenase (SDH), a series of pyrazole-4-carbohydrazides were rationally designed, synthesized, and characterized under the guidance of the structures of succinate dehydrogenase inhibitors (SDHIs). Bioassay results *in vitro* indicated that most of the target compounds exhibited excellent activity against *Rhizoctonia solani* (*R. solani*), *Fusarium graminearum* (*F. graminearum*), *Botrytis cinerea* (*B. cinerea*) and *Colletotrichum capsica* (*C. cinerea*). The compounds **7d**, **7l**, **7t** and **7x** were identified as the most promoting candidates, their anti-*F. graminearum* EC_{50} values were as low as 0.56, 0.47, 0.46 and 0.49 μg/mL, respectively, presenting the similar antifungal activity as that of the commonly used fungicide carbendazim (0.43 μg/mL). The 3D-QSAR models were built for a systematic structure-activity relationship profile to explore more potent pyrazole-4-carbohydrazides as novel fungicides. Molecular docking of **7d**, **7l** and **7r** with SDH was performed to reveal the binding modes in active pocket and analyze the interactions between the molecules and the SDH protein.

Background and Originality Content

The plant diseases due to phytopathogenic fungi have resulted in serious yield losses and significant economic and environmental impact on agricultural communities and whole countries.[1] Besides, mycotoxin accumulation in grain has affected food safety and endangered the health of human and animals. Succinate dehydrogenase (SDH), also known as mitochondrial complex II, [2] is the only integral membrane protein complex simultaneously involved in the tricarboxylic acid cycle[3] and the mitochondrial electron transport chain,[4] which catalyzes the oxidation of succinate to fumarate in the mitochondrial matrix.[5] SDH is widely found in the mitochondria of eukaryotic cells and a variety of prokaryotic cells, which provides electrons for their aerobic respiratory chains.[6,7] Succinate dehydrogenase inhibitors (SDHIs) combine with SDH's ubiquinone reduction site and disrupt mitochondrial respiration chain, thus leading to the fungal death,[8] which has a unique mechanism of action and has no cross-resistance with other types of fungicides, such as benzimidazoles, strobilurins and aminopyridines. Therefore, SDHIs are excellent candidates for overcoming fungicide resistance and improving plant disease control. As early as 1966, the launch of the fungicide carboxin started the research of succinate dehydrogenase inhibitor fungicides by pesticide workers.[9,10] With the development of furametpyr in 1997, the mechanism of action of SDHIs has attracted widespread attention from researchers,[11] and many new SDHI fungicides have been developed, such as fluxapyroxad,[12] penflufen[13] and isoflucypram (**Figure 1**).[13-14]

Strikingly, the similar mechanism of action of these fungicides has led to the suggestion that these structurally dissimilar substances possess common pharmacophores, which consists of carboxyl core and amide bond.[15] Thus, it can speculate that carboxylic amide pharmacophore is essential for binding with the active site of SDH and maintaining activity. In addition, carbohydrazide group can be considered as an ideal and completely competent surrogate for the amide group.[16] With convenient synthetic methods and excellent chemical/physical characteristics, carbohydrazide units have played a very important role in the field of agricultural chemistry, and also possessed a broad scope of pharmacological and biochemical activities, including insecticidal [17], antibacterial,[18,19] antiviral,[20] antitumor,[21] antimalarial,[22] antifungal,[23-24] anti-inflammatory,[25] and other extensive biological and physiological activity.[26-29] Carbohydrazide units have received more and more extensive attention and widely used as the frameworks in the molecular design of new antifungal agents. Wang et al. reported a series of triazole hydrazide compounds and found some products exhibited significant antifungal activities against the test plant pathogens.[30] Yu et al. introduced a hydrazide moiety into coumarin carboxylic acid to synthesize a series of hydrazide compounds that showed obvious activities against six plant pathogens.[31] Reino et al. designed and synthesized a variety of benzohydrazide derivatives and found that the derivatives had good antifungal activity.[32] Consequently, it is significant to research new fungicidal molecules with a carbohydrazide moiety.

3D-QSAR research reveals the mode of binding of drug molecules and biological macromolecules by calculating the physical and chemical properties and structural parameters of compounds, and predicts or explains the pharmacological activity of small organic molecules.[33-36] Therefore, based on the results of 3D-QSAR research, analyzing the characteristics of receptors or pharmacological targets, and rationally designing new drug molecules is a very important molecule design strategy. According to our previous investigation on the pyrazole derivatives and

corresponding 3D-QSAR model, we found that the positive charge groups and hydrogen bond acceptors are favored at hydrazone position to improve the antifungal activity (**Figure 1**).[37] Besides, the 5-chloropyrazole framework screened by previous work showed an important role in maintaining the antifungal activity. [37] These results prompted us to focus on the exploration of new intermediate bridges of the active molecular skeleton with a 5-chloropyrazole framework. Strikingly, the conjugated carbohydrazide structure has an electron donating effect and the carbonyl oxygen is a hydrogen bond acceptor, which may mean that the hydrazone group can be replaced with a hydrazide structure for effectively improving the antifungal activity of the compounds. In view of this, we combined the 5-chloropyrazole framework with a carbohydrazide moiety to design the desired high performance compounds as antifungal agents potentially targeting SDH (**Figure 1**). Molecular docking and structure activity relationship (SAR) studies were further conducted to validate the key structural characteristics responsible for their fungicidal potency.

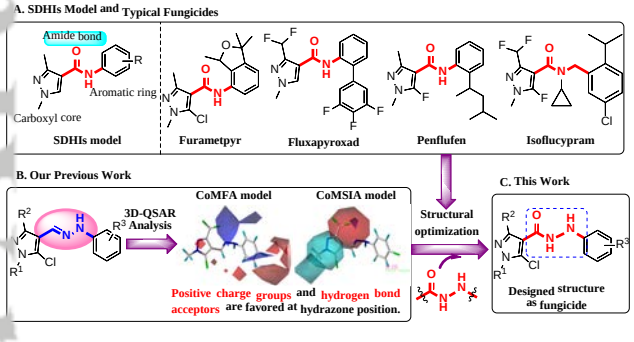

Figure 1. Design strategy for target molecules

Results and Discussion

Synthetic Chemistry

The synthetic approaches for the target compounds pyrazole-4-carbohydrazides **7a-7x** are shown in Scheme 1. The intermediates **4a-4c** were successfully achieved through cyclization and Vilsmeier-Haack-Arnold reaction, starting from diethyl malonate and ethyl acetoacetate, respectively. The compounds **4** were oxidized by potassium permanganate to provide 5-chloro pyrazole-4-carboxylic acids **5**. And then, the acids **5** were treated with thionyl chloride to give the acyl chloride intermediates **6**. Using triethylamine as the acid binding agent and dichloromethane as the reaction solvent, pyrazole-4-carbohydrazides **7a-7x** were expediently synthesized by the ammonolysis reaction of the intermediates **6** with substituted phenylhydrazines under 0 ℃ to room temperature. With the efficient methods, the structures of the target compounds were well supported by ^{1}H NMR, ^{13}C NMR, HRMS and IR analyses, and the structure of the typical compound **7j** was further confirmed by X-ray crystallographic diffraction analysis.

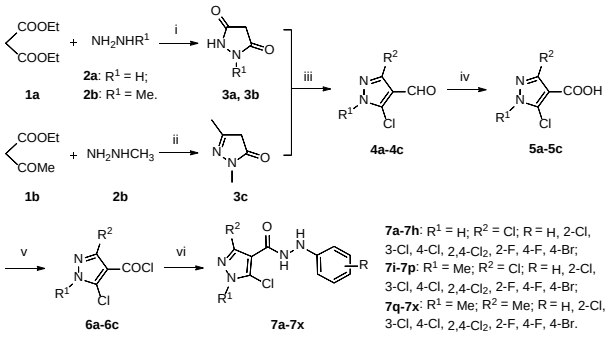

Scheme 1. Synthesis of target compounds **7a-7x**. Reagents and conditions: (i) EtOH, r.t., 8 h; EtONa (1.0 equiv.), EtOH, reflux, 6 h; 36% aq. HCl, pH = 1.0. (ii) EtOH, reflux, 6 h. (iii) $POCl_3$, DMF r.t. for 1 h, 55 ℃ for 2 h, then 110 ℃ for 5 h; NaOH, pH = 7.0. (iv) $KMnO_4$ (1.5 equiv), H_2O, reflux, 4 h; 36% aq. HCl, pH = 1.0. (v) $SOCl_2$, reflux, 6 h. (vi) Substituted phenylhydrazines with R group (1.0 equiv.), Et_3N (1.5 equiv.), CH_2Cl_2, 0 ℃, r.t., 12 h.

X-ray crystal structure of target compounds 7j

To actually confirm the structures of synthesized compounds, the molecular structure of target compound **7j** was studied as a representative example by single-crystal X-ray analysis shown in **Figure 2**. The crystal structure of **7j** was crystallized in the monoclinic crystal system, space group *P*21/c with a = 11.7349 (7) Å, b = 11.3262 (5) Å, c = 9.8434 (5) Å, α = 90°, β = 90.170 (5)°, γ = 90°, Z = 4, Dc = 1.624 g/cm^3, V = 1307.37 (12) Å3, total R indices: R_1 = 0.0499, $wR(F^2)$ = 0.1279. The crystallographic data have been deposited with the Cambridge Crystallographic Data Centre (CCDC) under a assigned number of CCDC 1846972.

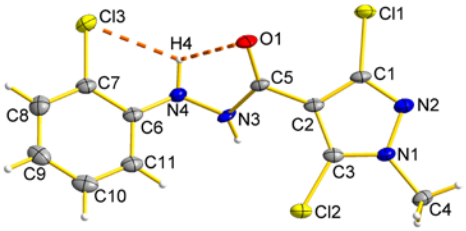

Figure 2. X-ray single crystal structure of compound **7j**

In vitro antifungal activity screening of target compounds

Table 1. Inhibition effects (%) of target compounds **7a-7x** against four test fungi at 10 μg/mL.[a]

Compd.	*F. graminearum*	*B. cinerea*	*R. solani*	*C. capsici*
7a	72.52±0.7	43.10±0.9	98.54±0.1	41.98±0.1
7b	48.30±0.3	24.94±1.1	95.62±0.3	83.33±0.6
7c	66.00±0.1	65.40±0.7	98.05±0.1	94.44±0.1
7d	89.80±0.9	66.09±1.6	85.16±2.1	95.68±0.1
7e	48.72±1.8	59.77±1.8	95.62±0.6	96.30±0.1

7f	61.19±2.0	40.23±2.0	96.59±0.1	92.59±0.5
7g	98.30±0.7	70.98±0.7	99.03±0.1	96.30±0.7
7h	87.25±0.6	62.64±1.5	75.67±2.6	83.02±0.8
7i	70.57±0.9	51.15±1.8	96.30±0.5	68.52±1.1
7j	5.94±1.1	16.95±2.5	90.02±1.1	96.91±0.4
7k	83.00±1.0	61.78±2.1	92.21±1.9	96.91±0.7
7l	96.88±0.1	72.99±1.5	81.51±2.1	95.06±0.1
7m	61.19±4.0	56.61±0.1	91.73±3.6	76.54±1.0
7n	67.14±0.1	33.62±2.6	89.54±3.2	94.14±0.6
7o	98.87±0.1	77.59±0.8	91.48±1.2	45.68±0.1
7p	83.00±0.6	64.66±0.7	64.72±2.7	78.70±0.7
7q	60.34±0.9	38.79±2.8	70.56±1.8	58.64±0.8
7r	7.640±3.7	10.06±3.7	54.26±2.1	95.06±1.0
7s	72.24±1.9	51.72±2.7	83.21±0.0	95.37±1.2
7t	86.40±0.7	64.37±1.2	71.29±0.9	66.98±1.7
7u	59.20±1.4	30.17±2.0	84.91±0.5	81.48±0.9
7v	51.56±2.0	25.57±1.7	63.26±1.8	89.81±0.1
7w	95.18±0.7	70.69±0.9	89.29±0.8	56.79±0.8
7x	81.87±0.9	62.07±0.1	68.37±0.0	61.11±1.2
Carbendazim	92.70±0.1	95.54±0.1	98.84±0.3	84.53±0.8

[a] Average of three replicates.

The *in vitro* bioassay results in Table 1 showed that most of the target compounds exhibited obvious antifungal activity against four test fungi at 10 μg/mL with carbendazim as the positive control. Among them, compounds **7c**, **7d**, **7g**, **7h**, **7k**, **7l**, **7p**, **7t** and **7x** had impressive antifungal activity with the inhibition rates ranging from 61.11% to 99.03%, the results indicated that derivatives with a 4-halogen phenyl such as 4-chlorophenyl (**7d**, **7l** and **7t**), 4-fluorophenyl (**7g**) and 4-bromophenyl (**7h**, **7p** and **7x**) had a broader fungicidal spectrum. On the contrary, the target compounds with 2-halogen phenyl such as 2-chlorophenyl (**7b**, **7j** and **7r**) and 2-fluorophenyl (**7f** and **7n**) displayed weaker fungicidal activities against *F. graminearum* and *B. cinerea*. In addition, most of the compounds displayed promising fungicidal activities against *R. solani* and *C. capsici* at 10 mg/L. Compounds **7c**, **7e**, **7f**, **7g**, **7j** and **7k** exhibited above 90% activity against both *R. solani* and *C. capsici*. Meanwhile, Table 1 also showed that the compounds **7g**, **7l**, **7o** and **7w** exhibited significant anti-*F. graminearum* effects at 10 μg/mL, with corresponding inhibition rates of 98.30, 96.88, 98.87 and 95.18%, which are better than that of carbendazim (92.70%).

Table 2. Actual EC_{50} and predicted pEC_{50} values of compounds **7a-7x** against *F. graminearum*

Compd.	Actual EC_{50} (μg/mL)	Actual pEC_{50}[b]	CoMFA		CoMSIA	
			Predicted pEC_{50}[b]	Residual	Predicted pEC_{50}[b]	Residual
7a	2.02	5.128	5.311	-0.183	5.322	-0.194
7b	2.67	5.059	5.103	-0.044	5.070	-0.011
7c	1.54	5.298	5.244	0.054	5.282	0.016
7d	0.56	5.736	5.639	0.097	5.666	0.07
7e[a]	2.96	5.060	5.099	-0.039	5.004	0.056
7f	1.99	5.162	5.066	0.096	5.088	0.074
7g	0.65	5.651	5.620	0.031	5.585	0.066
7h	0.71	5.692	5.703	-0.011	5.796	-0.104
7i[a]	2.65	5.033	5.159	-0.126	5.099	-0.066
7j	1.76	5.259	5.226	0.033	5.165	0.094
7k	1.58	5.306	5.393	-0.087	5.369	-0.063
7l	0.47	5.835	5.802	0.033	5.733	0.102
7m	0.95	5.571	5.571	0.000	5.503	0.068
7n	1.51	5.303	5.254	0.049	5.236	0.067
7o	0.60	5.706	5.750	-0.044	5.645	0.061
7p	0.66	5.739	5.842	-0.103	5.842	-0.103
7q[a]	2.94	4.954	5.103	-0.149	5.014	-0.06
7r[a]	6.15	4.687	4.588	0.099	4.819	-0.132
7s	1.11	5.430	5.329	0.101	5.374	0.056
7t	0.46	5.817	5.719	0.098	5.734	0.083
7u	1.46	5.359	5.510	-0.151	5.523	-0.164
7v	2.27	5.096	5.142	-0.046	5.248	-0.152
7w	0.63	5.649	5.685	-0.036	5.638	0.011
7x	0.49	5.846	5.748	0.098	5.839	0.007
Carbendazim	0.43	–	–	–	–	–

[a] Compounds in the test set. [b] $pEC_{50} = -\log (EC_{50} \times 10^{-3}/M)$ (M: molecular weight).

To further evaluate the fungicidal potency and probe the SAR of the novel pyrazole-4-carbohydrazide derivatives, their EC_{50} values were tested against *F. graminearum*, and the results were shown in Table 2. The results suggested that compounds **7d**, **7g**, **7h**, **7l**, **7m**, **7o**, **7p**, **7t**, **7w** and **7x** showed considerable antifungal activities against *F. graminearum,* with their EC_{50} values lower than 1 μg/mL. Among them, compounds **7d**, **7l**, **7t** and **7x** exhibited outstanding antifungal activity against *F. graminearum* with the EC_{50} values of 0.56, 0.47, 0.46 and 0.49 μg/mL, respectively, which comparable to carbendazim (0.43 μg/mL).

Although it is difficult to extract clear structure-activity relationships (SAR) from the presented biological data, some preliminary SAR rules were found and described below. First, compounds bearing a halogen at 4-position of the benzene ring, such as 4-F, 4-Cl and 4-Br groups, showed better fungicidal activities than their corresponding 2-position of benzene analogues. Second, the introduction of CH_3 at the 1 or 3-position of pyrazole ring was unfavourable to improve the biological activity of target compounds.

3D-QSAR Analysis

To understand and analyze the deeper relationship between the structure and the activity of the target compounds, the fungicidal activity against *F. graminearum* was selected for a 3D-QSAR study by building CoMFA and CoMSIA models. All target compounds were randomly divided into two sections including a training set with twenty compounds and a test set with four

compounds. The EC_{50} values (mol/L) of target compounds against *F. graminearum* were calculated as the negative logarithms of their EC_{50} values (pEC_{50} values) for building 3D-QSAR models and listed in Table 2. And all the training set molecules were aligned on the common core of compound **7t** with the best fungicidal activity against *F. graminearum*, which was used as the template shown in **Figure 3A**. **Figure 3B** showed the superimposed structures of the aligned training set. Partial least-square (PLS) analysis was performed to establish a linear relationship between the molecular fields and the activity of molecules. The statistical parameters were given in Table 3. As shown in Table 3, the steric and electrostatic properties were calculated for the CoMFA model (q^2 = 0.781, r^2 = 0.900), and the steric, electrostatic, hydrophobic, hydrogen bond donor and hydrogen bond acceptor properties were calculated for the CoMSIA model (q^2 = 0.787, r^2 = 0.878). The above q^2 and r^2 values met a validation criterion (q^2 > 0.5 and r^2 > 0.8) that indicated the reliable predictive accuracy of 3D-QSAR models. [33-36] Contour maps for the CoMFA and CoMSIA models were displayed in **Figure 4**. Actual and predicted pEC_{50} values for the training set and test set were reported in Table 2, and the correlation plots of CoMFA and CoMSIA models were shown in **Figure 5**.

Table 3. PLS statistics of CoMFA and CoMSIA 3D-QSAR models

PLS statistics	CoMFA	CoMSIA	Validation criteria
q^2 [a]	0.781	0.787	>0.5
r^2 [b]	0.900	0.878	>0.8
s [c]	0.093	0.099	
ONC [d]	3	2	
Steric [e]	0.558	0.018	
Electrostatic [f]	0.442	0.331	
Donor [g]		0.037	
Acceptor [g]		0.065	
Hydrophobic [h]		0.549	

[a] Cross-validated correlation coefficient from leave-one-out. [b] Noncross-validated correlation coefficient. [c] Standard error of estimate. [d] Optimum number of principal components. [e] Steric field contribution. [f] Electrostatic field contribution. [g] Donor and acceptor, of hydrogen bond fields contribution, respectively. [h] Hydrophobic field contribution.

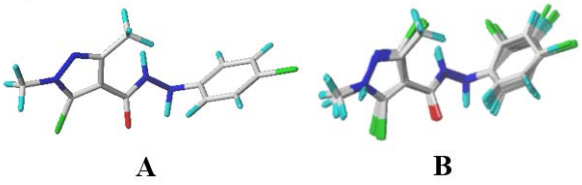

Figure 3. Alignment of all target compounds in the training set

The stereoscopic and electrostatic contour maps of CoMFA model were shown in **Figures 4A** and **4B**. The appearance of the green and red contours around 4-position of the benzene ring indicating bulky groups with a negative charge were favored at 4-position of the benzene ring to increase the antifungal activity. While, the yellow and blue contours around 2-position of the benzene ring indicated that bulky groups with a negative charge at this site were unfavorable to increase the antifungal activity. This observation is consistent with the fact that the compounds bearing a 4-ClPh (**7d**, **7l** and **7t**), 4-FPh (**7g**, **7o** and **7w**) or 4-BrPh (**7h**, **7p** and **7x**) group exhibit more obvious antifungal effects than these compounds bearing a 2-ClPh (**7b**, **7j** and **7r**), 2-FPh (**7f**, **7n** and **7v**) group or unsubstituted benzene ring (**7a**, **7i** and **7q**).

The stereoscopic and electrostatic contour maps of CoMSIA models were similar to the CoMFA models. While, it can be clearly seen that the green and yellow contours around 1 and 3-positions of the pyrazole ring in the CoMSIA models shown in **Figures 4C** and **4D**, which revealed that the introduction of a bulky group at the 1-position and a small group at the 3-position of the pyrazole ring could improve the antifungal activity.

In the CoMSIA hydrophobic contour map (**Figure 4E**), the yellow contour around the 4-position of the benzene ring indicated that the introduction of hydrophobic groups at this position were favored to increase the antifungal activity. The grey contour around 2-position of the benzene ring indicated that the introduction of hydrophobic groups here was not conducive to increase the activity. These results could be used to explain that the compounds bearing a 4-BrPh (**7h, 7p** and **7x**) group had better activity than the compounds bearing a 2-ClPh (**7b**, **7n** and **7r**) group.

The CoMSIA H-bond contour map (**Figure 4F**) showed that cyan contour around N-H group of hydrazide fragment suggested that hydrogen bond donor was favored in this area. While magenta contour around 1-position of the pyrazole ring indicated that the introduction of hydrogen bond acceptor could improve the activity.

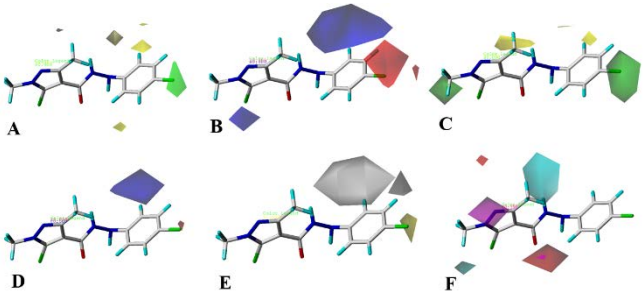

Figure 4. Contour maps of CoMFA and CoMSIA models

CoMFA model: (A) Sterically favored areas are in green, and sterically disfavored areas are in yellow; (B) Negative charge favored areas are in red and disfavored areas are in blue. CoMSIA model: The colors in (C) and (D) have the same meanings as the contour maps (A) and (B) of CoMFA model, respectively; (E) Hydrophobic favored areas are in yellow and disfavored areas are in gray; (F) Donor and acceptor favored areas are in cyan and magenta, respectively, and donor and acceptor disfavored areas are in purple and red, respectively.

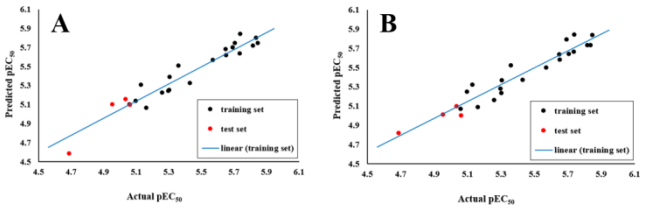

Figure 5. Correlations between CoMFA (A)/ CoMSIA (B) predicted and experimental pEC_{50}

Docking Analysis

To explore the possible and preliminary mechanism of the obvious antifungal activity and synthesized target compounds, we performed the molecular docking of highly fungicidal activity compounds **7d** and **7l** with SDH (PDB code 2FBW). The compound **7r** with a low fungicidal activity was included in the same investigation for comparison. To make the docking model more clear only major interactions were highlighted. Both **7d** and **7l** were embedded in the active pocket of SDH protein via the connection of hydrogen-bonding and hydrophobic interactions with some crucial amino acid residues including residues of tyrosine at 58 position (TYR58), tryptophan at 173 position (TRP173), proline at 169 position (PRO169), arginine at 43 position (ARG43), histidine at 216 position (HIS216), and isoleucine at 40 position (ILE40) (**Figure 6**). Compound **7d** and **7l** (**Figure 6A-6D**) showed three visible strong hydrogen bonds with the side chain amino acid residues of Tyr58 and Trp173, which play a crucial role in maintaining fungicidal activity. [38-39] In addition, the residues ARG43, HIS216, ILE40 and PRO169 also are critical in a continuous belt of hydrophobic interactions encircling pyrazole and benzene ring of compounds **7l** and **7d.** Obviously, compound **7r** (**Figure 6E** and **6F**) also showed strong interactions with SDH protein in the same active pocket and formed two hydrogen bonds with amino acid residues of Tyr58 and Trp173, which maintain its certain fungicidal activity. However, the same hydrophobic interactions were not observed in the docking model, and it can be clearly seen that the position of the benzene ring of compound **7r** is outside the above-mentioned amino acid residues, which could may greatly impair the fungicidal activity. Based on these results, it can be speculated that the designed compounds may serve as a novel type of SDH inhibitors.

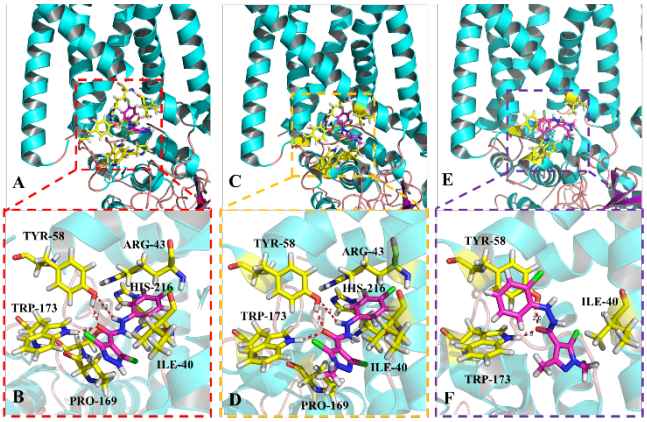

Figure 6 Molecular docking studies of compounds **7d** (A, B), **7l** (C, D) and **7r** (E, F). A-F were depicted using PyMol soft.

Conclusions

In summary, by introducing the carbohydrazide moiety at the 4-position of pyrazoles, a series of potential SDH inhibitors were designed, synthesized and well confirmed by IR, ^{1}H NMR, ^{13}C NMR, HRMS and single-crystal X-ray diffraction analyses. The bioassay results indicated that most target compounds showed remarkable antifungal activity against *R. solani*, *F. graminearum*, *B. cinerea* and *C. cinerea*. Strikingly. Nine target compounds **7c**, **7d**, **7g**, **7h**, **7k**, **7l**, **7p**, **7t** and **7x** had impressive antifungal activity against four test fungi at 10 μg/mL, with the inhibition rates ranging from 61.11% to 99.03%, which have a broader fungicidal spectrum. Compounds **7d**, **7l**, **7t** and **7x** exhibited significant antifungal activity against *F. graminearum*, with the EC_{50} values of 0.56, 0.47, 0.46 and 0.49 μg/mL, respectively, which are close to that of carbendazim (0.43 μg/mL). The 3D-QSAR model with good predictive accuracies revealed that introducing bulky groups with a negative charge at 4-position of benzene ring could effectively improve the activity against *F. graminearum*. The molecular docking study of compounds **7d**, **7l** and **7r** revealed the binding modes in active site, providing the preliminary evidence for target compounds as the SDH inhibitors. In line with the design expectation, introducing a carbohydrazide moiety into pyrazole framework was an effective structural modification to improve the antifungal activity. Given the structural novelty and significant fungicidal activity, the pyrazole-4-carbohydrazide derivatives are worthy of further structural optimization.

Experimental

Instruments and Materials

All reagents and solvents were obtained from commercial sources and used without further purification. Melting points were measured on an uncorrected WRS-1B digital melting point apparatus (Jingmi Science, China). ^{1}H NMR and ^{13}C NMR spectra were determined on a AV 400 MHz spectrometer (Bruker, Germany) using DMSO-d_6 as solvent and TMS as internal standard. Infrared spectra were recorded on a Nicolet 380 FT-IR

spectrometer (Thermo, America), and samples were prepared as KBr plates. HR-MS were acquired on a Triple TOF 5600 plus spectrometer (AB SCIEX, America). The progress of the reactions was monitored by thin layer chromatography (Yuhua, China).

General synthetic procedure for intermediates 5

The intermediates **4a**-**4c** were successfully prepared by the reported procedures with minor modifications[37]. The compound **4** (0.03 mol) was added in the solution of acetone (10 mL) and water (150 mL), and warmed to 60 ℃ with stirring. And then, potassium permanganate solid (7.1 g, 0.045 mol) was slowly added in portions and refluxed for 4 h. After the reaction was completed, the mixture was cooled, and 10% KOH aqueous solution was added to make the solution alkaline. After filtered, the filtrate was acidified with 36% hydrochloric acid until the pH = 1. A large amount of a white solid was precipitated, filtered, washed with water, and dried to give the white solid intermediate **5**.

General synthetic procedure for target compounds 7

The intermediate **5a** (4.0 g, 0.022 mol) was added in thionyl chloride (20 mL), and the mixture was refluxed for 6 h. After the reaction was completed, the excessive thionyl chloride was removed under reduced pressure to obtain the crude product **6a**. A solution of phenylhydrazine (0.27 g, 2.5 mmol) and dichloromethane (10 mL) was added dropwise in the mixture of **6a** (0.50 g, 2.5 mmol) and dichloromethane (10 mL) at 0 ℃. The mixture was stirred for 5 min, then Et_3N (0.38 g, 3.75 mmol) was added slowly. The reaction was performed at room temperature for 10 h. And the mixture was washed successively with 1M hydrochloric acid and water, desolvated, recrystallized with the mixed solvent of dichloromethane and petroleum ether (1: 4, V/V), and dried to obtain the target compound **7a.** Compounds **7b-7x** were synthesized using a similar method with substituted phenylhydrazine as one of the raw materials.

Single Crystal X-ray Diffraction Data Collection

The suitable crystal of compound **7j** was grown from dimethyl sulfoxide by the slow solvent evaporation method at room temperature. The single crystal X-ray diffraction was performed with a Bruker Smart APEX II CCD diffractometer. The crystal data of compound **7j** were measured with graphite-monochromatized Mo Kα radiation (λ = 0.71073 Å) at 296 (2) K. The crystal structure was solved by direct methods using SHELXS-97 and refined with SHELXL of the SHELXTL package.[36]

Biological Assays

The antifungal activities of the synthesized compounds were tested *in vitro* against *R. solani*, *F. graminearum*, *B. cinerea* and *C. cinerea* by a mycelium growth rate method, with carbendazim as the positive control. [33-35] The tested fungal strains were provided by the Laboratory of Plant Disease Control, Nanjing Agricultural University. The target compounds with inhibition rates exceeding 50% at the concentration of 10 μg/mL were further tested for their antifungal inhibition rates at five different concentrations to calculate the corresponding EC_{50} values.

QSAR Analyses and Molecular Docking

The three-dimensional (3D) QSAR and molecular docking were performed with the SYBYL X 2.0 program (Shanghai Tri-I. Biotech. Inc., China), using built-in QSAR software and Surflex-Dock, respectively. Three-dimensional structures of the title compounds were fully geometry-optimized using a conjugate gradient procedure based on the TRIPOS force field and Gasteiger-Hückel charges with a convergence criterion of 0.005 kcal/mol (Å). Partial least square (PLS) regression analysis was used to derive CoMFA and CoMSIA models. [33-35]

The crystal structure of SDH was downloaded from the RCSB Protein Data Bank (PDB code 2FBW). And the ligand (P/CBE 202) was extracted and all H_2O molecules were removed from the structure.[40]

Supporting Information

The supporting information for this article is available on the WWW under https://doi.org/10.1002/cjoc.2018xxxxx.

Acknowledgement

Authors gratefully acknowledge the grants from the National Natural Science Foundation of China (No. 31772209), the Fundamental Research Funds for the Central Universities of China (No. KYTZ201604) and the Postgraduate Research & Practice Innovation Program of Jiangsu Province (KYCX20_0562).

References

[1] Wang, Z.-J.; Gao, Y.; Hou, Y.-L; Zhang, C.; Yu, S.-J.; Bian, Q.; Li Z.-M.; Zhao, W.-G. Design, synthesis, and fungicidal evaluation of a series of novel 5-methyl-1*H*-1,2,3-trizole-4-carboxyl amide and ester analogues. *Eur. J. Med. Chem.* **2014**, *86*, 87-94.

[2] Zhu, X.-L.; Xiong, L.; Li, H.; Song, X.-Y.; Liu, J.-J.; Yang, G.-F. Computational and experimental insight into the molecular mechanism of carboxamide inhibitors of succinate-ubquinone oxidoreductase. *ChemMedChem.* **2014**, *9*, 1512-1521.

[3] Moosavi, B.; Berry, E. A.; Zhu, X.-L.; Yang, W.-C.; Yang, G.-F. The assembly of succinate dehydrogenase: a key enzyme in bioenergetics. *Cell. Mol. Life Sci.* **2019**, *76*, 4023-4042.

[4] Xiong, L.; Li, H.; Jiang, L.-N.; Ge, J.-M.; Yang, W.-C.; Zhu, X.-L.; Yang, G.-F. Structure-based discovery of potential fungicides as succinate ubiquinone oxidoreductase inhibitors. *J. Agric. Food Chem.* **2017**, *65*, 1021-1029.

[5] Sun, F.; Huo, X.; Zhai, Y.; Wang, A.; Xu, J.; Su, D.; Bartlam, M.; Rao, Z. Crystal structure of mitochondrial respiratory membrane protein complex II. *Cell.* **2005**, *121*, 1043-1057.

[6] Xiong, L.; Shen, Y.-Q.; Jiang, L.-N.; Zhu, X.-L.; Yang, W. C.; Huang, W.; Yang, G. F. Succinate dehydrogenase: an ideal target for fungicide discovery. *ACS Symposium Series.* **2015**, *1204*, 175-194.

[7] Xiong, L.; Zhu, X.-L.; Shen, Y.-Q.; Wishwajith, W. K. W. M.; Li, K.; Yang, G.-F. Discovery of N-benzoxazol-5-yl-pyrazole-4-carboxamides as nanomolar SQR inhibitors. *Eur. J. Med. Chem*. **2015**, 95, 424-434.

[8] Guo, X.; Zhao, B.; Fan, Z.; Yang, D.; Zhang, N.; Wu, Q.; Yu, B.; Zhou, S.; Kalinina, T. A.; Belskaya, N. P. Discovery of novel thiazole carboxamides as antifungal succinate dehydrogenase inhibitors. *J.*

Agric. Food Chem. **2019**, *67*, 1647-1655.
[9] Xiong, L.; Zhu, X.-L.; Gao, H.-W.; Fu, Y.; Hu, S.-Q.; Jiang, L.-N.; Yang W.-C., Yang, G.-F. Discovery of potent succinate-ubiquinone oxidoreductase inhibitors via pharmacophore-linked fragment virtual screening approach. *J. Agric. Food Chem.* **2016**, *64*, 4830-4837.
[10] DellaGreca, M.; Iesce, M. R.; Cermola, F.; Rubino, M.; Isidori, M. Phototransformation of carboxin in water. Toxicity of the pesticide and its sulfoxide to aquatic organisms. *J. Agric. Food Chem*. **2004**, *52*, 6228−6232.
[11] Chen, H.-S; Li, Z.-M. Synthesis of some heteroaryl pyrazole derivatives and their biological activities. *Chin. J. Chem*. **2000**, *18*, 596-602.
[12] Fernández-Ortuño, D.; Pérez-garcía, A.; Chamorro, M.; de la Peña, E.; De Vicente, A.; Torés, J. A. Resistance to the SDHI fungicides boscalid, fluopyram, fluxapyroxad, and penthiopyrad in *Botrytis cinerea* from commercial strawberry fields in Spain. *Plant Dis.* **2017**, *101*, 1306-1313.
[13] Umetsu, N.; Shirai, Y. Development of novel pesticides in the 21st century. *J. Pestic. Sci.* **2020**, *45*, 54-74.
[14] Desbordes, P.; Essigmann, B.; Gary, S.; Gutbrod, O.; Maue, M.; Schwarz, H.-G. Isoflucypram, the first representative of a new succinate dehydrogenase inhibitor fungicide subclass: its chemical discovery and unusual binding mode. *Pest Manag. Sci*. **2020,** *76*, 3340-3347.
[15] Zhang, A.; Zhou, J.; Tao, K.; Hou, T.; Jin, H. Design, synthesis and antifungal evaluation of novel pyrazole carboxamides with diarylamines scaffold as potent succinate dehydrogenase inhibitors. *Bioorg. Med. Chem. Lett*. **2018**, *28*, 3042-3045.
[16] Wu, Y.-Y.; Shao, W.-B.; Zhu, J.-J.; Long, Z.-Q.; Liu, L.-W.; Wang, P. Y.; Li, Z.; Yang, S. Novel 1,3,4-oxadiazole-2-carbohydrazides as prospective agricultural antifungal agents potentially targeting succinate dehydrogenase. *J. Agric. Food Chem*. **2019**, *67*, 13892-13903.
[17] Sun, J.; Zhou, Y. Design, synthesis, and insecticidal activity of some novel diacylhydrazine and acylhydrazone derivatives. *Molecules* **2015**, *20*, 5625-5637.
[18] Carvalho, S. A.; da Silva, E. F.; de Souza, M. V. N.; Lourenço, M. C. S.; Vicente, F. R. Synthesis and antimycobacterial evaluation of new *trans*-cinnamic acid hydrazide derivatives. *Bioorg. Med. Chem. Lett*. **2008**, *18*, 538-541.
[19] Muluk, M. B.; Phatak, P. S.; Pawar, S. B.; Dhumal, S. T.; Rehman, N. N.; Dixit, P. P.; Prafulla, B. C.; Haval, K. P. Synthesis, antimicrobial, and antioxidant activities of new pyridyl- and thiazolyl- bearing carbohydrazides. *J. Chin. Chem. Soc-Taip.* **2019**, *66*, 1507-1517.
[20] Giancotti, G.; Cancellieri, M.; Balboni, A.; Bassetto, M. Rational modifications on a benzylidene-acrylohydrazide antiviral scaffold, synthesis and evaluation of bioactivity against Chikungunya virus. *Eur. J. Med. Chem.* **2018**, *149*, 56-68.
[21] Grande, F.; Aiello, F.; De Grazia, O.; Brizzi, A.; Garofalo, A.; Neamati, N. Synthesis and antitumor activities of a series of novel quinoxalinhydrazides. *Bioorg. Med. Chem.* **2007**, *15*, 288-294.
[22] Soares, R. R.; da Silva, J. M. F.; Carlos, B. C.; da Fonseca, C. C.; de Souza, L. S. A.; Lopes, F. V.; de Paula Dias, R. M.; Moreira, P. O. L.; Abramo, C.; Viana, G. H. R.; de Pila Varotti, F.; da Silva, A. D.; Scopel, K. K. G. New quinoline derivatives demonstrate a promising antimalarial activity against *Plasmodium falciparum in vitro* and *Plasmodium berghei in vivo*. *Bioorg. Med. Chem. Lett*. **2015**, *25*, 2308-2313.
[23] Yan, T.; Yu, S.; Liu, P.; Liu, Z.; Wang, B.; Xiong, L.; Li, Z. Design, synthesis and biological activities of novel benzoyl hydrazines containing pyrazole. *Chin. J. Chem.* **2012**, *30*, 919-923.
[24] Xu, H.; Hou, Z.; Liang, Z.; Guo, M.-B.; Su, X.; Guo, C. Design, synthesis and antifungal activity of benzofuran and its analogues. *Chin. J. Chem.* **2019**, *37*, 1245-1250.
[25] Park, E. B.; Kim, K. J.; Jeong, H. R.; Lee, J. K.; Kim, H. J.; Lee, H. H.; Lim, J. W.; Shin, J.-S.; Koeberle, A.; Werz, O.; Lee, K.-T.; Lee, J. Y. Synthesis, structure determination, and biological evaluation of phenylsulfonyl hydrazide derivatives as potential anti-inflammatory agents. *Bioorg. Med. Chem. Lett*. **2016**, *26*, 5193-5197.
[26] Khattab, S. N. Synthesis and biological activity of novel amino acid-(*N*'-benzoyl) hydrazide and amino Acid-(*N*'-nicotinoyl) hydrazide derivatives. *Molecules.* **2005**, *10*, 1218-1228.
[27] Zhang, X.; Zhang, H.; Ma, J; Yu, S.; Li, Z. Design, synthesis and biological activities of novel *N*-aryl-1*H*-pyrazole-5-carboxylate derivatives. *Chem. Res. Chin. Univ.* **2019,** https://doi.org/10.1007/s40242-019-9274-3.
[28] Abdel-Aziz, H. A.; Elsaman, T.; Al-Dhfyan, A.; Attia, M. I.; Al-Aashood, K. A.; Al-Obaid, A.-R. M. Synthesis and anticancer potential of certain novel 2-oxo-*N*'-(2-oxoindolin-3-ylidene)-2*H*-chromene-3-carbohydrazides. *Eur. J. Med. Chem*. **2013**, *70*, 358-363.
[29] Khan, I.; Tantray, M. A.; Hamid, H.; Alam, M. S.; Kalam, A.; Dhulap, A. Synthesis of benzimidazole based thiadiazole and carbohydrazide conjugates as glycogen synthase kinase-3β inhibitors with anti-depressant activity. *Bioorg. Med. Chem. Lett*. **2016**, *26*, 4020-4024.
[30] Wang, X.; Dai, Z.-C.; Chen, Y.-F.; Cao, L.-L.; Yan, W.; Li, S.-K.; Wang, J.-X.; Zhang, Z.-G.; Ye, Y.-H. Synthesis of 1,2,3-triazole hydrazide derivatives exhibiting anti-phytopathogenic activity. *Eur. J. Med. Chem.* **2017**, *126*, 171-182.
[31] Yu, X.; Teng, P.; Zhang, Y.-L.; Xu, Z.-J.; Zhang, M.-Z.; Zhang, W.-H. Design, synthesis and antifungal activity evaluation of coumarin-3-carboxamide derivatives. *Fitoterapia.* **2018**, *127*, 387-395.
[32] Reino, J. L.; Saiz-Urra, L.; Hernandez-Galan, R.; Aran, V. J.; Hitchcock, P. B.; Hanson, J. R.; Gonzalez, M. P.; Collado, I. G. Quantitative structure-antifungal activity relationships of some benzohydrazides against *Botrytis cinerea*. *J. Agric. Food Chem*. **2007**, *55*, 5171-5179.
[33] Si, W.-J.; Wang, X.-B.; Chen, M.; Wang, M.-Q.; Lu, A.-M.; Yang, C.-L. Design, synthesis, antifungal activity and 3D-QSAR study of novel pyrazole carboxamide and niacinamide derivatives containing benzimidazole moiety. *New J. Chem*. **2019**, *43*, 3000-3010.
[34] Wang, X.; Hu, H.; Zhao, X.; Chen, M.; Zhang, T.; Geng, C.; Mei, Y.; Lu, A.; Yang, C. Novel quinazolin-4 (3*H*)-one derivatives containing a 1,3,4-oxadiazole thioether moiety as potential bactericides and fungicides: Design, synthesis, characterization and 3D-QSAR analysis. *J. Saudi Chem. Soc*. **2019**, *23*, 1144-1156.
[35] Wang, X.; Wang, M.; Yan, J.; Chen, M.; Wang, A.; Mei, Y; Si, W.; Yang, C. Design, synthesis and 3D-QSAR of new quinazolin-4(3*H*)-one derivatives containing a hydrazide moiety as potential fungicides. *ChemistrySelect.* **2018**, *3*, 10663-10669.
[36] Chen, J.; Gan, X.; Yi, C.; Wang, S.; Yang, Y.; He, F.; Hu, D.; Song, B. Synthesis, nematicidal activity, and 3D-QSAR of novel 1,3,4-oxadiazole/ thiadiazole thioether derivatives. *Chin. J. Chem.* **2018**, *36*,

939-944.

[37] Jiao, J.; Wang, A.; Chen, M.; Wang, M.-Q.; Yang, C.-L. Novel 5-chloro-pyrazole derivatives containing a phenylhydrazone moiety as potent antifungal agents: synthesis, crystal structure, biological evaluation and a 3D-QSAR study. *New J. Chem*. **2019**, *43*, 6350-6360.

[38] Yang, D.; Zhao, B.; Fan, Z.; Yu, B.; Zhang, N.; Li, Z.; Zhu, Y.; Zhou, J.; Kalinina, T. A.; Glukhareva, T. V. Synthesis and biological activity of novel succinate dehydrogenase inhibitor derivatives as potent fungicide candidates. *J. Agric. Food Chem*. **2019**, *67*, 13185-13194.

[39] Liu, H.; Xia, D.-G.; Hu, R.; Wang, W.; Cheng, X.; Wang, A.-L.; Lv, X.-H. A bioactivity-oriented modification strategy for SDH inhibitors with superior activity against fungal strains. *Pestic. Biochem. Phys.* **2020**, *163*, 271-279.

[40] Li, S.; Li, D.; Xiao, T.; Zhang, S.; Song, Z.; Ma, H. Design, synthesis, fungicidal activity, and unexpected docking model of the first chiral boscalid analogues containing oxazolines. *J. Agric. Food Chem*. **2016**, *64*, 8927-8934.

(The following will be filled in by the editorial staff)
Manuscript received: XXXX, 2019
Manuscript revised: XXXX, 2019
Manuscript accepted: XXXX, 2019
Accepted manuscript online: XXXX, 2019
Version of record online: XXXX, 2019

Entry for the Table of Contents

Page No. 8

Title Synthesis, Bioactivity Evaluation, 3D-QSAR, and Molecular Docking of Novel Pyrazole-4-carbohydrazides as Potential Fungicides Targeting Succinate Dehydrogenase

Jian Jiao, Min Chen, Shengxin Sun, Weijie Si, Xiaobin Wang, Weijie Ding, Xincan Fu, An Wang, Chunlong Yang*

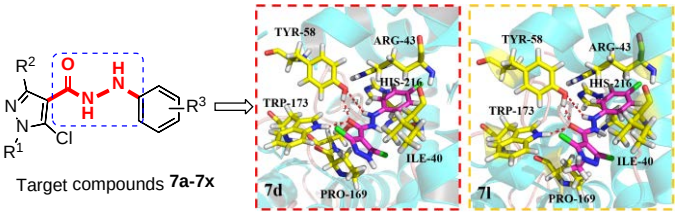

Target compounds **7a-7x**

Antifungal activities against *F. graminearum*:
7d: R^1 = H, R^2 = Cl, R^3 = 4-Cl. EC_{50} = 0.56 ug/mL;
7l: R^1 = Me, R^2 = Cl, R^3 = 4-Cl. EC_{50} = 0.47 ug/mL.

The compounds **7d** and **7l** were identified as the most promoting fungicide candidates against *F. graminearum* with the comparable antifungal EC_{50} values (0.56 and 0.47 μg/mL) to that of carbendazim (0.43 μg/mL). Compound **7d** and **7l** showed three visible strong hydrogen bonds with the side chain amino acid residues of Tyr58 and Trp173, which play a crucial role in maintaining fungicidal activity.

[a] *Department, Institution, Address 1*
E-mail:

[b] *Department, Institution, Address 2*
E-mail:

[c] *Department, Institution, Address 3*
E-mail: